Journal of Materials Chemistry B

ROYAL SOCIETY OF CHEMISTRY

PAPER

View Article Online
View Journal | View Issue

Cite this: J. Mater. Chem. B, 2022, 10, 7563

An antioxidant nanodrug protects against hepatic ischemia–reperfusion injury by attenuating oxidative stress and inflammation†

Shuai Zhang,[a] Yue Cao,[d] Bo Xu,[d] Hao Zhang,[c] Songtao Zhang,[c] Jian Sun,*[a] Ying Tang *[b] and Yinghui Wang *[c]

Liver transplantation is currently recognized as the only effective therapeutic option for end-stage liver disease. Hepatic ischemia–reperfusion injury (IRI) remains a major cause of graft damage or dysfunction, and is mediated by the abundant production of reactive oxygen species (ROS) and a complex cascade of inflammation during the reperfusion period. However, no universal antioxidant has been applied in clinical practice due to its low bioavailability and non-specific targeting. Herein, cerium oxide and manganese oxide nanocomposites (CM NCs), with the advantages of high biocompatibility, passive liver-targeting and short-term metabolic excretion, were synthesized as a nanodrug for hepatic IRI therapy. The CM NCs exhibited excellent superoxide dismutase (SOD) and catalase (CAT) mimetic activity to scavenge ROS and generate oxygen (O_2). Therefore, CM NCs could alleviate oxidative stress, subsequently suppress the activation of Kupffer cells (KCs) and neutrophils, and reduce the secretion of inflammatory factors due to the synergistic effect of ROS scavenging and O_2 production. By exploring the underlying mechanisms of the CM NCs in the treatment of hepatic IRI, we suggest that the CM NCs with ROS scavenging and inflammation regulation capacity show clinical potential for hepatic IRI management and provide new perspectives in the treatment of other oxidative-stress-related diseases.

Received 6th December 2021,
Accepted 21st March 2022

DOI: 10.1039/d1tb02689e

rsc.li/materials-b

[a] Department of Cardiovascular Center, The First Hospital of Jilin University, 71 Xinmin Street, Changchun 130021, Jilin, China. E-mail: sun_jian@jlu.edu.cn
[b] Department of Gastroenterol, The First Hospital of Jilin University, 71 Xinmin Street, Changchun 130021, Jilin, China. E-mail: tuboshu123@jlu.edu.cn
[c] State Key Laboratory of Rare Earth Resource Utilization, Changchun Institute of Applied Chemistry (CIAC), Chinese Academy of Sciences, Changchun, Jilin, 130022, China. E-mail: yhwang@ciac.ac.cn
[d] The First Hospital of Jilin University, 71 Xinmin Street, Changchun 130021, Jilin, China

† Electronic supplementary information (ESI) available. See https://doi.org/10.1039/d1tb02689e

Ying Tang

Ying Tang received her PhD degree in internal medicine from Jilin University in 2017. She is working as attending physician at the First Hospital of Jilin University. Her research interest focus on synthesis and bioapplication of multifunctional nanomaterials.

Introduction

Ischemia–reperfusion injury (IRI) is a major pathophysiologic mechanism involved in many clinical states, such as acute myocardial infarction,[1] stroke,[2] organ transplantation[3] and intraoperative cessation of the blood supply.[4] Currently, liver transplantation, as the only effective treatment option for end-stage liver disease,[5] has evolved rapidly with advances in immunosuppressive management and surgical techniques.[6] However, hepatic IRI remains a well-recognized major cause of graft dysfunction and hepatic failure after surgical procedures.[7] During the reperfusion period, significant reactive oxygen species (ROS) such as hydrogen peroxide (H_2O_2), hydroxyl radicals ($^{\bullet}OH$) and superoxide anions ($^{\bullet}O_2^-$) can induce DNA damage, lipid peroxidation and cell necrosis, which initiates a further inflammation cascade and aggravates liver-tissue damage.[8–10] Thus, as critical initiators of oxidative stress and inflammatory response, ROS have been a potential target for antioxidant therapies.[11]

Despite extensive research that has confirmed the effectiveness of antioxidants (alpha-lipoic acid,[12] *N*-acetylcysteine[13] and curcumin[14]) in alleviating IRI, their clinical application has been immensely hampered due to their poor aqueous solubility, low bioavailability and non-specific targeting. Along with

the overwhelming development of nanotechnology, taking advantage of the inherently excellent properties of nanomaterials, including small size, high surface area and tunable surfaces for functionalization with biomolecules,[15,16] various nanomaterials with antioxidant activities have been being explored in oxidative-stress-related diseases including atherosclerosis,[17] stroke,[18–20] acute kidney injury[21] and chronic inflammatory diseases.[22,23] However, non-specific uptake and the elimination of most nanoparticles *via* the reticuloendothelial system (RES, *e.g.*, liver, spleen) have consistently been barriers to effective tissue-targeted delivery *in vivo*.[15] Using this imperfect preferential uptake enrichment of the liver, nano-antioxidants have shown promising applications in hepatic IRI treatment. However, as far as we know, research on exploring the nano-antioxidants for alleviating hepatic IRI remains in the early stages.[24–27] In addition, hypoxia is an important critical factor that can promote the expression of pro-inflammatory factors.[28] It has been demonstrated that oxygen (O_2) replenishment can reduce the pro-inflammatory macrophage level and prevent inflammation-induced tissue necrosis in a drug-induced liver injury model.[29] Therefore, it is highly desirable to design and construct a nanodrug with the capacity for scavenging ROS and generating oxygen, which could hold promise in facilitating the therapeutic efficiency of hepatic IRI.

Herein, we first synthesized a novel bovine serum albumin (BSA)-functionalized nanocomposite based on cerium oxide and manganese oxide (CM NCs) for the therapy of hepatic IRI (Scheme 1). Due to the transition between Ce^{3+} and the Ce^{4+} oxidation state,[30,31] CeO_2 can catalyze ($^{\bullet}O_2^-$) to produce H_2O_2 and remove ($^{\bullet}OH$) *via* superoxide dismutase (SOD) mimetics and redox reactions, respectively. MnO_2 can further decompose H_2O_2 and exhibits a high O_2-production efficiency due to its catalase (CAT)-like activity. During the reperfusion period, the CM NCs demonstrated a good performance in reducing the levels of oxidative stress, decreasing Kupffer cell (KC) activation, diminishing the release of inflammatory factors (*i.e.*, tumor necrosis factor-α (TNF-α), interleukin-1β (IL-1β), interleukin-6 (IL-6) and interferon gamma-γ (IFN-γ)), and restricting neutrophil recruitment and infiltration in a hepatic IRI model, all of which can be ascribed to the synergistic effect of ROS scavenging and O_2 generation. Therefore, all findings demonstrate that CM NCs are promising nanodrugs for the treatment of hepatic IRI, and provide new perspectives in the management of other oxidative-stress-related diseases.

Results and discussion

Synthesis and characterization of CM NCs

CM NCs were fabricated through biomineralization. As shown in the transmission electronic microscopy (TEM) image (Fig. 1a), the as-prepared ultrasmall CM NCs with an average

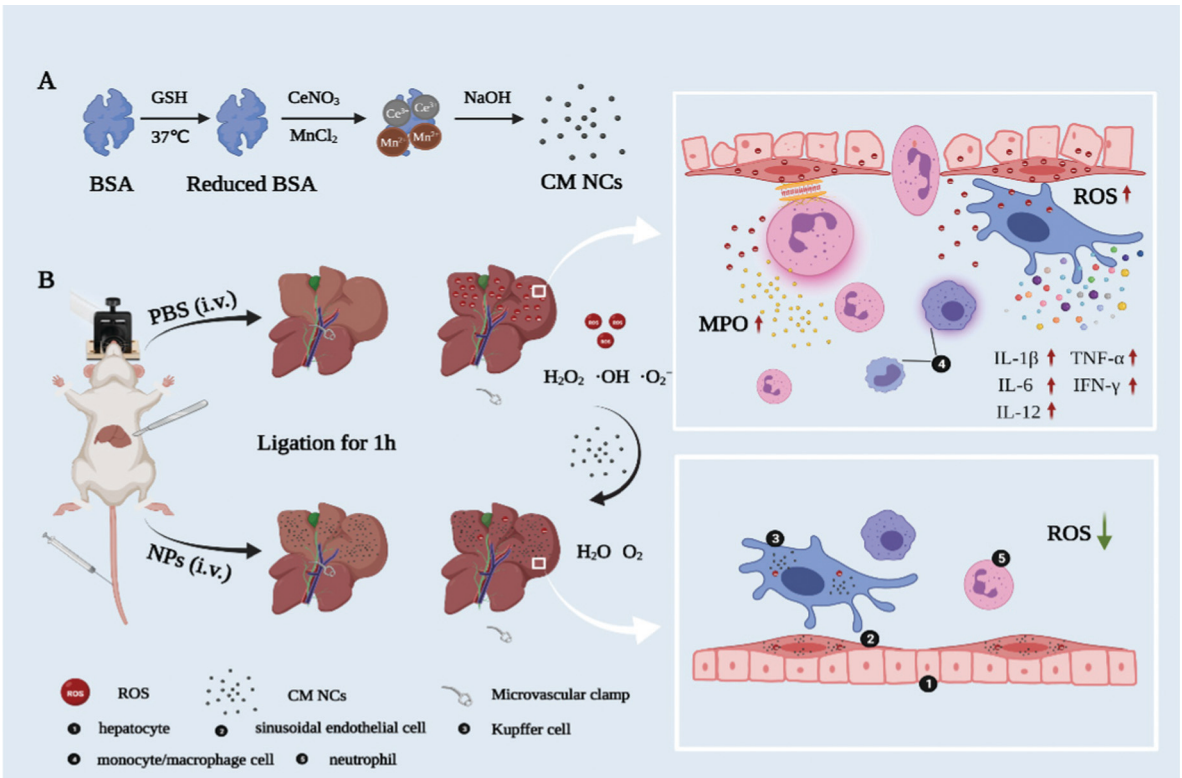

Scheme 1 A. Synthetic procedures of CM NCs. B. Schematic illustration of the therapeutic mechanisms of CM NCs. The CM NCs can scavenge and eliminate $^{\bullet}O_2^-$, H_2O_2, and $^{\bullet}OH$ during the reperfusion process, subsequently suppressing the activation of Kupffer cells and neutrophils, and reducing the secretion of inflammatory factors. ROS, reactive oxygen species; IL-1β, interleukin-1β; TNF-α, tumor necrosis factor-α; IL-6, interleukin-6; IL-12, interleukin-12; IFN-γ, interferon gamma-γ; MPO, myeloperoxidase.

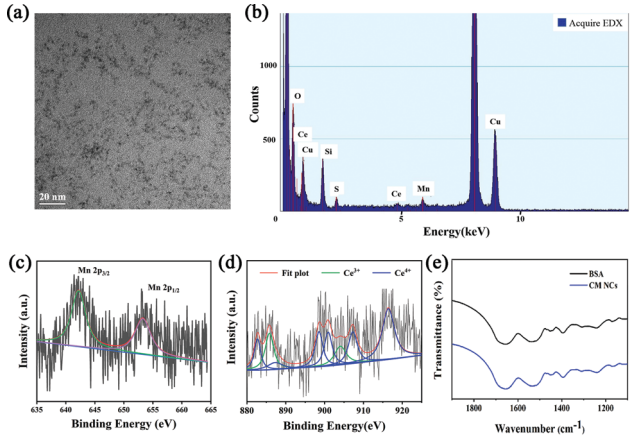

Fig. 1 Characterization of CM NCs. (a) TEM image of CM NCs. (b) EDX spectroscopy of CM NCs. (c and d) XPS spectra corresponding to (c) Mn and (d) Ce of the CM NCs. (e) FT-IR spectra of BSA and CM NCs.

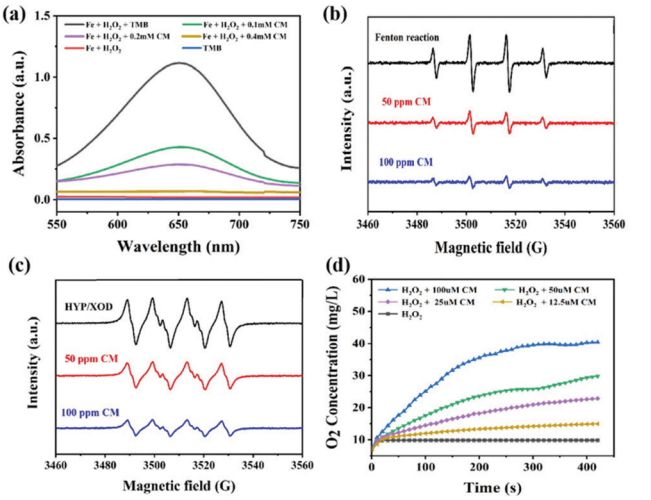

Fig. 2 ROS-scavenging properties of CM NCs. (a) Absorption spectra of TMB after reaction with Fe^{2+}/H_2O_2, in the absence and presence of CM NCs. (b and c) ESR spectra of $^{\bullet}OH$ and $^{\bullet}O_2^-$, respectively, using DMPO as the spin trap agent, with the addition different concentrations of CM NCs. (d) Generation of oxygen from different concentrations of CM NCs with H_2O_2. The concentration of CM NCs is expressed in the form of the molar concentration of Ce.

size of about 2 nm showed uniform morphology and good monodispersity. Energy dispersive X-ray spectroscopy (EDX) (Fig. 1b) confirmed the existence of Ce, Mn and O, which is consistent with the result of the energy dispersive spectrometer (EDS)-elemental mapping (Fig. S1, ESI†). X-Ray photoelectron spectroscopy (XPS) revealed characteristic peaks at 642.5 and 654.0 eV, which corresponded to $Mn2p_{3/2}$ and $Mn2p_{1/2}$ of MnO_2. The XPS spectrum also showed the binding energy levels of Ce(III) (885.7 and 904.0 eV) and Ce(IV) (882.7, 887.2, 898.5, 900.9, 907.2 and 916.4 eV), which confirmed the existence of the mixed-valence state of Ce^{3+} and Ce^{4+} in the CM NCs with Ce^{4+} being dominant (Fig. 1c and d and Fig. S2, ESI†). It is known that higher ratios of Ce^{3+}/Ce^{4+} exhibit a higher SOD-like activity, and higher levels of Ce^{4+} sites show significant CAT-like activity.[32,33] Thus, the CM NCs not only scavenge $^{\bullet}O_2^-$ but also remove the H_2O_2 generated in the SOD-mimetic process. The results of X-ray diffraction (XRD; Fig. S3, ESI†) of the CM NCs also confirmed their successful synthesis. The FT-IR spectra indicated the successful modification of BSA on the surface of the nanocomposite (Fig. 1e). Owing to the existence of BSA, the CM NCs showed great dispersity in water with the average hydrodynamic size of 23.12 nm (Fig. S4, ESI†). Moreover, the zeta potential of CM NCs was −18.67 mV (Fig. S5, ESI†), and the CM NCs showed good colloidal stability with no significant change in the particle size distribution for at least 7 days (Fig. S6, ESI†).

ROS scavenging properties of CM NCs

To evaluate the ROS-scavenging activities of the CM NCs, such as the hydroxyl radical ($^{\bullet}OH$) scavenging activity, the SOD-mimicking activity and the CAT-mimicking activity, UV-vis absorbance spectroscopy, electrospin resonance (ESR) spectra and the oxygen production were monitored, respectively (Fig. 2). First, the $^{\bullet}OH$ generated by Fenton reaction with the Fe^{2+}/H_2O_2 was detected using the specific probe 3,3′,5,5′-tetramethylbenzidine (TMB). After mixing TMB with Fe^{2+}/H_2O_2, an obvious absorption peak at 650 nm was observed (Fig. 2a). After adding CM NCs to the Fe^{2+}/H_2O_2 system, the intensity of the absorption peak progressively decreased with the increase in the CM NC concentration. Furthermore, the $^{\bullet}OH$ scavenging capacity of the CM NCs was confirmed by ESR spectra. As shown in Fig. 2b, the 1 : 2 : 2 : 1 multiple peak intensity indicated the amount of $^{\bullet}OH$, that was captured by 5,5′-dimethylpyrroline-1-oxide (DMPO). The signal of DMPO/$^{\bullet}OH$ diminished with the addition of CM NCs. Similarly, the scavenging of $^{\bullet}O_2^-$ by the CM NCs was also assessed *via* ESR spectroscopy using DMPO as a spin trap (Fig. 2c). The $^{\bullet}O_2^-$ was generated by the hypoxanthine/xanthine oxidase (HYP/XOD) system that served as a control group. The DMPO/$^{\bullet}OOH$ signal intensity decreased as the concentration of CM NCs was increased, indicating their ability to eliminate $^{\bullet}O_2^-$. To test the H_2O_2 decomposition capacity of the CM NCs, the amount of generated O_2 was monitored using a dissolved-oxygen meter. Compared with the control group (only H_2O_2), the amount of O_2 production and the rate of O_2 release evidently increased with an increasing CM NC concentration (Fig. 2d). All the results above demonstrated that CM NCs have an excellent capacity for scavenging ROS and generating O_2.

Intracellular ROS scavenging by CM NCs

For subsequent bioapplications, a compatibility assessment was first performed using a standard Cell Counting Kit-8 (CCK-8) assay. No significant cytotoxicity for human hepatocarcinoma (HepG2) cells and human embryonic kidney 293T (HEK293T) cells was observed (Fig. S8, ESI†), even if the CM NC concentration reached 1500 μg mL^{-1}. Moreover, the CM NCs do not cause any obvious hemolysis, even at a concentration of 1500 μg mL^{-1}, when co-cultured with mouse red blood cells (Fig. S9, ESI†). The cellular uptake of CM NCs by mouse

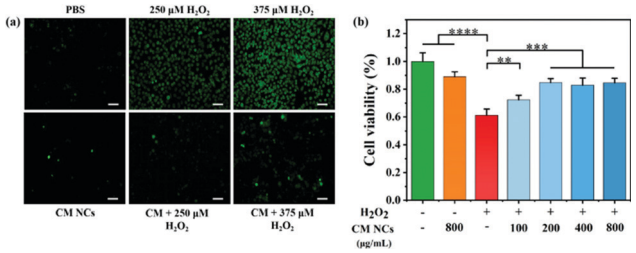

Fig. 3 (a) Fluorescent staining images of HepG2 cells treated with CM NCs using HPF for ROS staining. Scale bar: 50 μm. (b) *In vitro* cell viabilities of HepG2 cells treated with different concentrations of CM NCs in the absence and presence of H_2O_2. Data represent the mean ± s.d.; *P* values were calculated *via* two-tailed Student's *t*-test, $*P < 0.05$; $**P < 0.01$; $***P < 0.001$; $****P < 0.0001$.

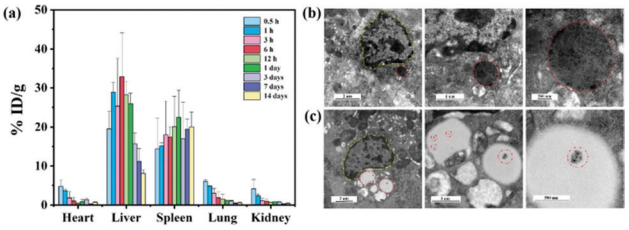

Fig. 4 *In vivo* biodistribution of CM NCs. (a) Biodistributions of Ce element in the main organs at various time points. (b and c) Bio-TEM images of mouse liver tissue demonstrating the uptake of CM NCs in the Kupffer cells and hepatic astrocytes after intravenous injection of CM NCs. The yellow dashed line in (b) outlines the nucleus of the KC and the red dotted circle indicates lysosome within the engulfed CM NCs. The yellow dashed line in (c) shows the nucleus of the astrocyte and the red dotted circle highlights the CM NCs in lipid droplets.

macrophages (RAW264.7) increased with the duration of incubation (Fig. S10, ESI†). Then, hydroxyphenyl fluorescein (HPF) was selected as a fluorescence probe to assess the intracellular ROS-scavenging capability of the CM NCs. After incubation with a culture medium containing different concentrations of H_2O_2 (250 μM or 375 μM), HepG2 cells showed green fluorescence, indicating the generation of ROS in HepG2 cells, as shown in Fig. 3a. When the CM NCs were added to an H_2O_2-containing cell system, the green fluorescence intensity showed a distinct weakening, confirming the good scavenging capability of the CM NCs. By contrast, for PBS only and the CM NC group, no significant fluorescence signal was observed. The ROS scavenging ability was further quantified by monitoring the cell viability after adding 1 mM H_2O_2 and different concentrations of CM NCs, ranging from 100 to 800 μg mL^{-1}. Fig. 3b shows that the cell viability of HepG2 cells improved with an increasing concentration of CM NCs, indicating their good scavenging ability. The good biocompatibility and superior ROS scavenging activity endow the CM NCs with good potential for the treatment of hepatic IRI.

In vivo biodistribution and biocompatibility of CM NCs

The liver is a major organ involved in macromolecule metabolism, distribution and elimination.[34] Mostly, nanomaterials can be trapped by KCs and achieve passive enrichment in the liver through intravenous (i.v.) injection.[35] In particular, nanomaterials with a negative surface charge are more susceptible to be phagocytosed by KCs.[36,37] To quantify the biodistribution of the CM NCs, inductively-coupled plasma-atomic emission spectroscopy (ICP-AES) was employed to detect the content of Ce at various time points post-i.v.-injection. As shown in Fig. 4a, the CM NCs were predominantly taken up by the RES, such as the liver and spleen, and were significantly enriched in the liver at 6 hours after tail-vein injection. Due to their small particle diameter, the CM NCs traveled quickly to the liver, but were also gradually metabolized and eliminated from the liver 24 hours after administration. Up to 14 days, a very small amount of Ce element was detected in the liver tissue. To observe the cellular uptake of CM NCs after their intravenous injection, liver tissue was prepared for bio-transmission electron microscopy (bio-TEM). And as visualized *via* bio-TEM (Fig. 4b), the CM NCs were phagocytized mainly by the KCs. This might partially be due to the CM NCs with a negative surface charge being more likely to be taken up by KCs.[38] Moreover, we also observed the aggregation of CM NCs in the lipid droplets of hepatic astrocytes. Thereby, both of these advantages, including a passive liver targeting ability and short-term metabolic excretion, make the CM NCs ideal for the treatment of hepatic IRI.

For further assessment of the biocompatibility of the CM NCs *in vivo*, healthy ICR mice were randomly divided into two groups, as a PBS-treated group and a CM NCs-treated group. The serum biochemical markers of the two groups, which included ALT, AST, alkaline phosphatase (ALP), albumin and blood urea nitrogen (BUN), were evaluated. No statistical difference was found between the two groups (Fig. S11, ESI†). Meanwhile, the blood parameters (Fig. S12, ESI†) and hematoxylin–eosin (H&E) staining of the main organs (Fig. S13, ESI†) appeared to show no obvious toxicity 30 days after receiving the CM NC treatment. Thus, the CM NCs exhibit excellent biocompatibility in both the short and long term.

Prevention of hepatic IRI with CM NCs

For the *in vivo* study, all mice were separated randomly into six groups, and included a healthy group, a CM NC-treated group, a sham group, a hepatic IRI group, a 12 h- and a 7 day-group after IRI mice had been treated with CM NC. The hepatic IRI model was established according to a previous protocol.[39] In the sham group, the mice underwent the same surgical procedures except ligation. The serum biochemical markers (ALT and AST) are the main indicators of hepatic function in clinical assessments and experiment research.[40] At 12 h and 7 days, respectively, after surgery, the serum ALT and AST levels were monitored to assess the short- and long-term protective effects of CM NCs for IRI. Compared with the healthy group, the ALT and AST levels of the IRI mice were significantly higher (Fig. 5a and b), which suggests a severely impaired liver function. For the group of CM NC-treated IRI mice, both indicators were found to be slightly elevated at 12 h post-surgery. Moreover, both ALT and AST levels at 7 days after treatment with the CM NCs had returned to the healthy level. These results indicated

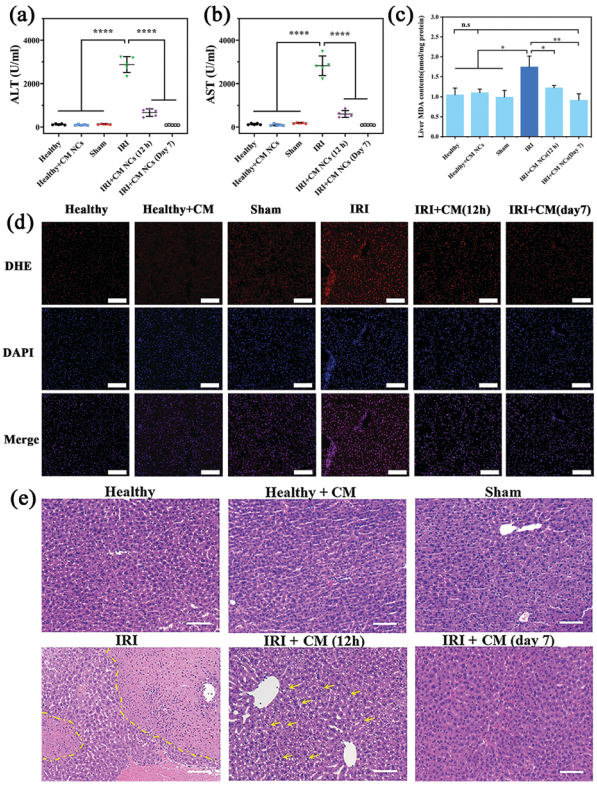

Fig. 5 Prevention of hepatic IRI with CM NCs. Indicator levels of hepatic function included (a) ALT and (b) AST from each group. (c) MDA levels in liver homogenates from each group. (d) Images of fluorescent staining of liver tissues with DHE and 4,6-diamidino-2-phenylindole (DAPI). Scale bar: 100 μm. (e) H&E staining of the liver tissue of each group. The dashed yellow lines outline severe damage areas with hepatocellular necrosis, hemorrhage and inflammatory cells. The yellow arrows indicate hepatocyte cytoplasm vacuolization. Scale bar: 100 μm. Data represent the mean ± s.d.; *P* values were calculated *via* two-tailed Student's *t*-test, $*P < 0.05$; $**P < 0.01$; $***P < 0.001$; $****P < 0.0001$.

that hepatic damage was alleviated through treatment with CM NCs.

ROS at physiologically low levels play a significant role in intracellular signal transduction and maintain a redox balance in the organism.[41] ROS overproduction can result in oxidative stress, which causes lipid peroxidation and cell membrane damage.[42] So $^{\bullet}O_2^-$ levels in the liver tissues from each group were detected by fluorescent staining using dihydroethidium (DHE). As shown in Fig. 5d, the red fluorescence intensities of the treated groups were significantly reduced compared with the IRI group, which further confirmed the ROS scavenging activity of the CM NCs *in vivo*. In addition, malondialdehyde (MDA), a product of lipid peroxidation, has been widely used as one of the indicators of oxidative stress. The MDA levels of hepatic tissue homogenates in each group were detected. As shown in Fig. 5c, the level of MDA in IRI mice was markedly increased compared with the other groups. By contrast, for the IRI mice with CM NC treatment, the MDA levels remained close to the mice of the healthy group. Such a result provides direct evidence that the CM NCs can reduce oxidative stress and alleviate liver tissue injury.

The H&E staining of liver tissue was performed for further pathological evaluation. Severe liver injury was significantly observed in IRI mice receiving PBS treatment (Fig. 5e). The area marked by the dashed yellow line showed a large area of hepatic cell necrosis and hemorrhage. However, a milder liver injury with some hepatocyte cytoplasm vacuolization (marked with yellow arrows) was found in the CM NCs-treated IRI group. After treatment with CM NCs for 7 days, the hepatic tissue morphology showed no visible damage and no difference from the healthy group. All these results further confirmed that the CM NCs can effectively prevent hepatic IRI.

Regulating the inflammatory process of hepatic IRI

Hepatic IRI is a complex pathological and physiological phenomenon involving multiple mechanisms. In addition to the direct oxidative damage caused by oxidative stress, as another important mechanism, the inflammatory response that is triggered by excessive ROS and hypoxia can exacerbate liver damage.[28,43,44] KCs, which are liver tissue-specific macrophages, are activated by damage-associated molecular pattern (DAMP) molecules such as high mobility group box 1 (HMGB1), thereby inducing further production of ROS and the release of numerous pro-inflammatory cytokines.[45] For a more comprehensive understanding of how the CM NCs exert their protective effects, enzyme-linked immunosorbent assay (ELISA) was conducted to assess the levels of several cytokines secreted in the liver homogenates. The pro-inflammatory cytokine IL-1 exhibited significantly elevated levels in the PBS-treated IRI group compared with the healthy mice, as shown in Fig. 6b. Moreover, IL-1β has the potential to increase TNF-α synthesis and release by the KCs.[46] As a central role in hepatic IRI, TNF-α can stimulate the activation of monocytes/macrophages,[47] but it can also promote the release of other cytokines, such as IL-6.[48] However, the above cytokine levels were markedly downregulated for the CM NC-treated IRI group due to the ROS scavenging activity of the CM NCs (Fig. 6a–c).

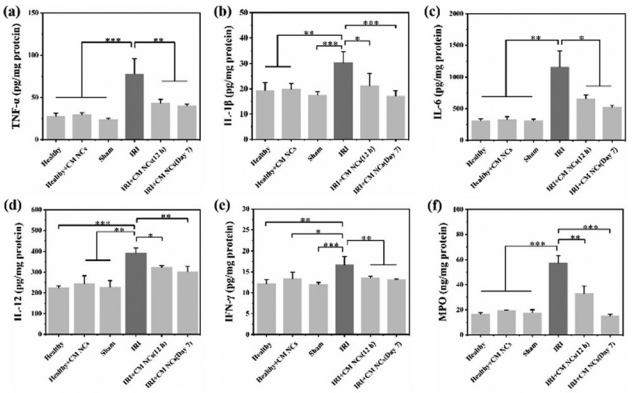

Fig. 6 CM NCs regulate the inflammatory process of hepatic IRI. (a–f) The cytokines TNF-α (a), IL-1β (b), IL-6 (c), IL-12 (d), IFN-γ (e), and MPO (f) were detected in liver homogenates from each group *via* ELISA. Data represent the mean ± s.d.; *P* values were calculated *via* two-tailed Student's *t*-test, $*P < 0.05$; $**P < 0.01$; $***P < 0.001$; $****P < 0.0001$.

In addition to ROS production and the release of pro-inflammatory cytokines, activated KCs also secrete chemokines that induce the recruitment and activation of neutrophils, resulting in further aggravation of hepatic IRI.[43,49] IL-1β, TNF-α, IL-12 and IFN-γ are the key cytokines secreted by activated KCs to promote migration, adhesion, accumulation and activation of neutrophils.[50,51] From Fig. 6a, b, d and e, it was confirmed that the secretion of these cytokines was highly increased. Activated neutrophils, as the main actor of tissue damage, exacerbate liver reperfusion injury by releasing numerous ROS and several proteolytic enzymes.[52] Myeloperoxidase (MPO), a neutrophil-specific peroxidase enzyme and a biomarker of neutrophil infiltration, is released into the extracellular environment when neutrophils are activated and degranulated. According to Fig. 6f, we observed an increased neutrophil accumulation, as demonstrated by the increased MPO activity in the IRI group. Nevertheless, the mice with the CM NC treatment could significantly decrease the expression of MPO in hepatic IRI. As such, the CM NCs have a great potential in the prevention of hepatic IRI *via* scavenging the ROS produced by KCs, decreasing KCs and monocyte/macrophage activation, regulating inflammatory cytokine secretion and reducing neutrophil recruitment.

Conclusions

In conclusion, CM NCs with a small size and high biocompatibility were successfully synthesized and used for the treatment of hepatic IRI. The CM NCs exhibited excellent SOD and CAT mimetic activities to scavenge and eliminate $^{\bullet}O_2^-$, H_2O_2, and $^{\bullet}OH$. Moreover, *in vitro* experiments confirmed that the ROS-scavenging activities of CM NCs could protect cells against oxidative stress damage. Further *in vivo* studies demonstrated that CM NCs effectively restored the SOD levels and alleviated liver injury during the hepatic IRI process. Importantly, we further demonstrated that the CM NCs significantly alleviate oxidative stress during the reperfusion process, subsequently suppressing the activation of KCs and neutrophils, and reducing the secretion of inflammatory factors. In summary, the CM NCs, with the advantages of small size, high biocompatibility, and passive liver-targeting ability, have the capacity to scavenge ROS and regulate inflammation, and could be a potential nanodrug for the treatment of hepatic IRI. Moreover, our study also provides the foundation for further investigations, for the application of CM NCs in the treatment of other oxidative-stress-related diseases.

Conflicts of interest

There are no conflicts to declare.

Acknowledgements

This work was supported by grants from the National Natural Science Foundation of China (81770374).

Notes and references

1 E. T. Chouchani, V. R. Pell, E. Gaude, D. Aksentijevic, S. Y. Sundier, E. L. Robb, A. Logan, S. M. Nadtochiy, E. N. J. Ord, A. C. Smith, F. Eyassu, R. Shirley, C. H. Hu, A. J. Dare, A. M. James, S. Rogatti, R. C. Hartley, S. Eaton, A. S. H. Costa, P. S. Brookes, S. M. Davidson, M. R. Duchen, K. Saeb-Parsy, M. J. Shattock, A. J. Robinson, L. M. Work, C. Frezza, T. Krieg and M. P. Murphy, *Nature*, 2014, **515**, 431–435.
2 T. Kahles, P. Luedike, M. Endres, H. J. Galla, H. Steinmetz, R. Busse, T. Neumann-Haefelin and R. P. Brandes, *Stroke*, 2007, **38**, 3000–3006.
3 I. Prieto and M. Monsalve, *Redox Biol.*, 2017, **12**, 1020–1025.
4 R. F. van Golen, M. J. Reiniers, P. B. Olthof, T. M. van Gulik and M. Heger, *J. Gastroenterol. Hepatol.*, 2013, **28**, 394–400.
5 A. Parente, D. C. Osei-Bordom, V. Ronca, M. Perera and D. Mirza, *Front. Immunol.*, 2020, **11**, 565616.
6 W. Zhang, M. Wang, H. Y. Xie, L. Zhou, X. Q. Meng, J. Shi and S. Zheng, *Transplant. Proc.*, 2007, **39**, 1332–1337.
7 Z. Li, Y. Wang, Y. Zhang, X. Wang, B. Gao, Y. Li, R. Li and J. Wang, *Arch. Med. Res.*, 2021, **52**, 163–173.
8 W. A. Dar, E. Sullivan, J. S. Bynon, H. Eltzschig and C. Ju, *Liver Int.*, 2019, **39**, 788–801.
9 T. Yoshitomi and Y. Nagasaki, *Adv. Healthcare Mater.*, 2014, **3**, 1149–1161.
10 G. Katwal, D. Baral, X. Fan, H. Weiyang, X. Zhang, L. Ling, Y. Xiong, Q. Ye and Y. Wang, *Oxid. Med. Cell. Longevity*, 2018, **2018**, 2976957.
11 I. Andreadou, P. Efentakis, K. Frenis, A. Daiber and R. Schulz, *Basic Res. Cardiol.*, 2021, **116**, 44.
12 N. Ambrosi, D. Guerrieri, F. Caro, F. Sanchez, G. Haeublein, D. Casadei, C. Incardona and E. Chuluyan, *Int. J. Mol. Sci.*, 2018, **19**, 102.
13 W. Chen and D. Li, *Front. Chem.*, 2020, **8**, 732.
14 S. G. Ibrahim, S. Z. El-Emam, E. A. Mohamed and M. F. Abd Ellah, *Int. Immunopharmacol.*, 2020, **80**, 106131.
15 J. Bourquin, A. Milosevic, D. Hauser, R. Lehner, F. Blank, A. Petri-Fink and B. Rothen-Rutishauser, *Adv. Mater.*, 2018, **30**, e1704307.
16 H. Wei and E. Wang, *Chem. Soc. Rev.*, 2013, **42**, 6060–6093.
17 H. Kim, S. Kumar, D. W. Kang, H. Jo and J. H. Park, *ACS Nano*, 2020, **14**, 6519–6531.
18 T. Mei, A. Kim, L. B. Vong, A. Marushima, S. Puentes, Y. Matsumaru, A. Matsumura and Y. Nagasaki, *Biomaterials*, 2019, **215**, 119209.
19 L. Z. He, G. N. Huang, H. X. Liu, C. C. Sang, X. X. Liu and T. F. Chen, *Sci. Adv.*, 2020, **6**, eaay9751.
20 G. Huang, J. Zang, L. He, H. Zhu, J. Huang, Z. Yuan, T. Chen and A. Xu, *ACS Nano*, 2022, **16**, 431–452.
21 Z. T. Rosenkrans, T. Sun, D. Jiang, W. Chen, T. E. Barnhart, Z. Zhang, C. A. Ferreira, X. Wang, J. W. Engle, P. Huang and W. Cai, *Adv. Sci.*, 2020, **7**, 2000420.
22 J. Kim, H. Y. Kim, S. Y. Song, S. H. Go, H. S. Sohn, S. Baik, M. Soh, K. Kim, D. Kim, H. C. Kim, N. Lee, B. S. Kim and T. Hyeon, *ACS Nano*, 2019, **13**, 3206–3217.

23 J. Wu, Y. Yu, Y. Cheng, C. Cheng, Y. Zhang, B. Jiang, X. Zhao, L. Miao and H. Wei, *Angew. Chem., Int. Ed.*, 2021, **60**, 1227–1234.
24 D. Ni, H. Wei, W. Chen, Q. Bao, Z. T. Rosenkrans, T. E. Barnhart, C. A. Ferreira, Y. Wang, H. Yao, T. Sun, D. Jiang, S. Li, T. Cao, Z. Liu, J. W. Engle, P. Hu, X. Lan and W. Cai, *Adv. Mater.*, 2019, **31**, e1902956.
25 X. Zhang, J. Hu, K. V. Becker, J. W. Engle, D. Ni, W. Cai, D. Wu and S. Qu, *J. Nanobiotechnol.*, 2021, **19**, 107.
26 J. Y. Kim, D. Y. Lee, S. Kang, W. Miao, H. Kim, Y. Lee and S. Jon, *Biomaterials*, 2017, **133**, 1–10.
27 Y. Long, H. Wei, J. Li, M. Li, Y. Wang, Z. Zhang, T. Cao, C. Carlos, L. G. German, D. Jiang, T. Sun, J. W. Engle, X. Lan, Y. Jiang, W. Cai and X. Wang, *Nano Lett.*, 2020, **20**, 6510–6519.
28 H. K. Eltzschig and P. Carmeliet, *New Engl. J. Med.*, 2011, **364**, 656–665.
29 F. Li, Y. Qiu, F. Xia, H. Sun, H. Liao, A. Xie, J. Lee, P. Lin, M. Wei, Y. Shao, B. Yang, Q. Weng and D. Ling, *Nano Today*, 2020, **35**, 100925.
30 A. Dhall and W. Self, *Antioxidants*, 2018, **7**, 97.
31 I. Celardo, J. Z. Pedersen, E. Traversa and L. Ghibelli, *Nanoscale*, 2011, **3**, 1411–1420.
32 X. Liu, J. Wu, Q. Liu, A. Lin, S. Li, Y. Zhang, Q. Wang, T. Li, X. An, Z. Zhou, M. Yang and H. Wei, *J. Mater. Chem. B*, 2021, **9**, 7238–7245.
33 C. Xu and X. Qu, *NPG Asia Mater.*, 2014, **6**, e90.
34 S. A. Cummer, J. Christensen and A. Alu, *Nat. Rev. Mater.*, 2016, **1**, 1–13.
35 J. Panyam and V. Labhasetwar, *Adv. Drug Delivery Rev.*, 2003, **55**, 329–347.
36 K. Poelstra, J. Prakash and L. Beljaars, *J. Controlled Release*, 2012, **161**, 188–197.
37 S. H. Cheng, F. C. Li, J. S. Souris, C. S. Yang, F. G. Tseng, H. S. Lee, C. T. Chen, C. Y. Dong and L. W. Lo, *ACS Nano*, 2012, **6**, 4122–4131.
38 Y. Guan, W. Yao, K. Yi, C. Zheng, S. Lv, Y. Tao, Z. Hei and M. Li, *Small*, 2021, **17**, e2007727.
39 F. Chen, S. Goel, H. F. Valdovinos, H. M. Luo, R. Hernandez, T. E. Barnhart and W. B. Cai, *ACS Nano*, 2015, **9**, 7950–7959.
40 J. H. D. A. van Beek, M. H. M. de Moor, E. J. C. de Geus, G. H. Lubke, J. M. Vink, G. Willemsen and D. I. Boomsma, *Behav. Genet.*, 2013, **43**, 329–339.
41 E. Owusu-Ansah and U. Banerjee, *Nature*, 2009, **461**, 537–541.
42 E. H. Ruder, T. J. Hartman, J. Blumberg and M. B. Goldman, *Hum. Reprod. Update*, 2008, **14**, 345–357.
43 E. E. Montalvo-Jave, T. Escalante-Tattersfield, J. A. Ortega-Salgado, E. Pina and D. A. Geller, *J. Surg. Res.*, 2008, **147**, 153–159.
44 S. P. Li, F. F. Wang, W. K. Zhang, M. Z. Bian, S. Y. Zhang, H. Yan, Y. Fang and H. M. Zhang, *Inflammation*, 2019, **42**, 2139–2147.
45 H. Jaeschke and A. Farhood, *Am. J. Physiol.*, 1991, **260**, G355–G362.
46 N. Shirasugi, G. Wakabayashi, M. Shimazu, A. Oshima, M. Shito, S. Kawachi, T. Karahashi, Y. Kumamoto, M. Yoshida and M. Kitajima, *Transplantation*, 1997, **64**, 1398–1403.
47 A. E. Feldstein, N. W. Werneburg, A. Canbay, M. E. Guicciardi, S. F. Bronk, R. Rydzewski, L. J. Burgart and G. J. Gores, *Hepatology*, 2004, **40**, 185–194.
48 K. R. Mccurry, D. A. Campbell, W. E. Scales, J. S. Warren and D. G. Remick, *J. Surg. Res.*, 1993, **55**, 49–54.
49 M. Cannistra, M. Ruggiero, A. Zullo, G. Gallelli, S. Serafini, M. Maria, A. Naso, R. Grande, R. Serra and B. Nardo, *Int. J. Surg.*, 2016, **33**(Suppl 1), S57–S70.
50 N. Teoh, J. Field and G. Farrell, *J. Hepatol.*, 2006, **45**, 20–27.
51 X. D. Shen, B. Ke, Y. Zhai, F. Gao, S. I. Tsuchihashi, C. R. Lassmon, R. W. Busuttil and J. W. Kupiec-Weglinski, *Liver Transplant.*, 2007, **13**, 1435–1443.
52 R. Anaya-Prado, L. H. Toledo-Pereyra, A. B. Lentsch and P. A. Ward, *J. Surg. Res.*, 2002, **105**, 248–258.